Asia-Pac. J. Atmos. Sci., 53(1), 1-18, 2017
DOI:10.1007/s13143-016-0028-6
pISSN 1976-7633 / eISSN 1976-7951

Advances in Fog Microphysics Research in China

Duanyang Liu[1], Zihua Li[2], Wenlian Yan[1], and Yi Li[3]

[1]*Jiangsu Meteorological Observatory, Nanjing, China*
[2]*Key Laboratory for Aerosol-Cloud-Precipitation of China Meteorological Administration, Nanjing University of Information Science and Technology, Nanjing, China*
[3]*Department of Atmospheric Science, Colorado State University, Fort Collins, CO, USA*

(Manuscript received 8 March 2016; accepted 6 June 2016)

Abstract: Fog microphysical research in China based on field experiments obtained many important results in recent 50 years. With the fast development of China's economy, urbanization in the last 30 years, special features of fog microphysical structure also appeared, which did not appear in other countries. This article reviews the fog microphysical research around China, and introduces the effect of urbanization on fog microphysical structure and the microphysical processes as well as macroscopic conditions of radiation fog droplet spectral broadening. Urbanization led to an increase in fog droplet number concentration but decreases in fog liquid water content (LWC) and fog droplet size, as well as a decrease in visibility in large cities. Observations show that the radiation fog could be divided into wide-spectrum one, which is all extremely dense fog with the spectral width more than 40 μm, and narrow-spectrum one, most of which is dense fog with the spectral width less than 22 μm, according to droplet spectral distribution. During developing from dense fog to extremely dense fog, the wide-spectrum radiation fog is characterized by explosive deepening, that is, within a very short time (about 30 min), the droplet concentration increase by about one order of magnitude, droplet spectral broadening across 20 μm, generally up to 30-40 μm, or even 50 μm. As a result, water content increased obviously, visibility decreased to less than 50 m, when dense fog became extremely dense fog.

Key words: Fog microphysics, China, droplet spectral broadening, urbanization effect

1. Introduction

Fog microphysics is the study of micro-scale physical processes related to fog. Fog sciences include nucleation, condensation, growth of droplets, ice crystals, fog droplet settlement, and other microscopic physical processes. The study aimed at understanding the formation of fog, development and dissipation regulation grasping the variation trend, in order to issue warning as early as possible, avoid fog damage that may occur. Great importance of fog study has been well recognized in China (Li, 2001) since artificial weather modification was first carried out in 1958. The earliest cloud and fog observations were conducted on high mountains in 1958.

In 1959, the China Meteorological Administration Observatory and Institute of Lushan Mountain Weather Control observed cloud drops' spectrum and water content using hand-operated spectrometer in Lushan (Li, 2001). In 1960-1962, cloud and fog physics observation studies were carried out in Mt Hengshan (Gu, 1962; Gu and Hu, 1962; Gu and Zhan, 1962, 1964; Xu and Gu, 1963; Zhou, 1963; Zhou and Gu, 1963) and Mt Taishan by many researchers at the Institute of Geology, Chinese Academy of Sciences. Meanwhile, cloud and fog droplet spectrum and water content were observed using home-made "triplex droplet collector". The earliest city fog observation was conducted in Shanghai in the late 1950s and early 1960s (Li, 2001), during which the fog microstructure was analyzed using a fog droplet colletor.

In 1968 and 1969, there was a census of fog in southern China, in which preliminary observations were conducted on the microstructures of fog in Yunnan, Guizhou, Sichuan, Anhui, Zhejiang, Fujian, and Guangdong provinces (Li, 2001). Since the reform and opening of China and the development of national economy, fog hazard has become more and more prominent. The study of fog is of particular importance for all levels of government, and the observation of fog has undergone significant development. Comprehensive observations of fog have been conducted in Chengdu Shuangliu Airport of Sichuan Province (Guo et al., 1989), Zhoushan of Zhejiang Province, Xishuangbanna of Yunnan Province (Huang, 1992, 2001), Shanghai, and Chongqing. In addition to observing the microstructures of fog, fog boundary layer and fog water chemical compositions were also observed, to comprehensively study fog physical and chemical processes. Meanwhile, in Beijing (Zhang et al., 2005), Tianjin (Wu et al., 2008, 2010) and Xinjiang (Dilnur et al., 2008), observations of ice fog were also undertaken. In recent years, the fog observations plans included Nanling Dayaoshan Highway of Guangdong Province (Deng et al., 2002, 2007a, 2007b; Wu et al., 2005, 2006, 2007a, 2007b) and Nanjing of Jiangsu Province (Li et al., 2011a, 2011b; Liu, 2011; Liu et al., 2011, 2012a, 2016; Lu et al., 2008, 2010a, 2010b, 2011; Niu et al., 2010a, 2010b, 2012; Pu et al., 2008; Yang et al., 2009, 2010a, 2010b, 2012), Beijing (Jia and Guo, 2012; Ma et al., 2012), and the South China Sea (Lu et al., 2014a, 2014b; Yue et al., 2012, 2013, 2014; Zhang et al., 2013; Zhao et al., 2013). In particular, most of the recent fog observations were comprehensively conducted, including

Corresponding Author: Duanyang Liu, Jiangsu Meteorological Observatory, NO.2, Beijige, Nanjing, China.
E-mail: liuduanyang2001@126.com

macro- and micro-structures, fog water chemical characteristics, components of radiation and heat balance, turbulence structures of fog, as well as water vapor flux, heat flux, aerosol particle spectrum, and aerosol particle chemical composition, in addition to regular meteorological and environmental monitoring.

In China, the observations, analyses, and studies of fog microphysical structures over the years have resulted in many important results. The characteristics of fog microphysical structures have been determined, and the physical processes of fog formation and extinction have been further elucidated. At the same time, the theoretical studies have kept pace with field experiments and studies. As early as 1962, Gu (1962) proposed 15 equations of cloud and fog physics, which can be used to thoroughly study fog formation and development. These scientific results and insights are highly advanced. After the 1970s, numerical models of fog have been gradually developed (Huang and Guo, 1986; Zhou, 1987; Sun et al., 1991; Zhang and Li, 1993; Shi et al., 1997, 2001; Huang et al., 2000; Fu, 2002; Fan et al., 2004; Zhou et al., 2004; Dong et al., 2006), to simulate microphysical processes of fog and to discuss the correlations between fog and some other factors. The fog numerical models have undergone several different phases, from one-dimensional numerical model (Huang and Guo, 1986) to two-dimensional time-integral numerical model (Sun et al., 1991; Zhang and Li, 1993), and then 3D model (Shi et al., 1997, 2001; Huang et al., 2000; Fu, 2002). In recent years, the mesoscale model were developed in fog forecast, such as MM5 (Fan et al., 2004; Dong et al., 2006), RAMS (Fu et al., 2004), and WRF (Teng et al., 2014). Different microphysics was joined in these numerical models.

Over the past 50 years, microphysical observations and experimental studies of fog in China have achieved many important outcomes and revealed the features about microscopic and macroscopic structures of various types of fog in China. In recent years, with the development of China's economy and society, some microphysical features of urban fog appeared that are rarely seen in other countries. Since most of the documents were published in Chinese, this review will summarize these previous studies.

In this review, we pay particular attention to fog microphysics research in China in the past 50 years. Measurement methods are presented in Section 2. Fog microphysical structures are reviewed in Section 3, and urbanization impacts are presented in Section 4. The radiation fog droplet spectral widening is discussed in Section 5, and fog-haze conversion is presented in Sections 6. The other studies of fog microphysics are reviewed in Section 7. Finally, conclusions and prospects are given in Section 8.

2. Measurement methods and classification of fog types

a. measurement methods

Methods of observing fog droplet spectrum are divided into direct and indirect measurements. Direct measurement is to sample fog droplets and then magnify them with a microscope, with a direct inspection followed by photographic acquisition. The triplex droplet collector that has been used for a long time for fog observations in China belongs to this category. The triplex droplet collector is mainly composed of a miniature wind tunnel and a sampling system. A strip-shaped droplet spectral sampling sheet passes at a constant velocity through the uniform fog-containing droplet flow in the wind tunnel, and the fog droplets settle onto a glass plate coated with oil (vaseline and transformer oil). Then, the sample is observed under the microscope to derive the size and number of fog droplets. The measurement scale ranges from 3.2 to 70 μm. Because the sampling plate has a different capability to capture fog droplets of different sizes in the airflow, it must correct the capture coefficient in order to derive the actual fog droplet spectral distribution. If it uses the jet sampling head instead at the entrance of the wind tunnel and uses calibrated absorbent paper for sampling, the fog droplets striking the absorbent paper will form water spots. According to the size of the water spots, we can infer the fog LWC. Usually, sampling of fog droplet spectrum is conducted every 5-10 min. Each sampling time is 0.1-0.5 s, and the error is $\leq \pm$ 10%. Since the temporal resolution of the triplex droplet collector is relatively low, the number of samples acquired during the fog process is relatively small, and it is difficult to record detailed information on fog during its occurrence, development and dissipation processes. These data can only reflect the general features of microphysical structures of fog and cannot capture subtle changes of these microphysical processes. In addition, the triplex droplet collector is fortuitous in the capture of large droplets (Deng et al., 2007b).

The indirect measurement method measures the extinction effect produced by fog droplets. The laser backscattering fog droplet spectrometer, first used by Nanjing University of Information and Technology at the end of 2006, is an example of this type (Liu et al., 2010a; Li et al., 2011a, 2011b). This type of fog droplet spectrometer includes an optical base, a signal processor, and a vacuum part that is used to remove dust particles passing through the optical window. The optical receiver receives the backscattering light of particles, which passes through the optical window, and the information processor converts the light pulse into voltage, which is then amplified and filtered to transmit to the data processing system. Because fog droplets of different sizes have varying laser scattering intensities, the optical receiver distributes the number of fog droplets into classes and calculates the number of fog droplets in each class. It also records the corresponding real-time airflow rate, pressure and temperature. This instrument can continuously measure the concentration and spectral distribution of fog droplets, and the particle size range is 2-50 μm, with a maximum concentration of 104 per cm^3. The advantage of this type of fog droplet spectrometer is continuous measurement during fog process, which generates one set of data every second (Liu et al., 2010a, 2011; Yang et al.,

Fig. 1. Sites of fog observations in China. ●: Mountain stations, ■: urban stations and ▲: coast stations.

2010b; Li et al., 2011a, 2011b). In addition to the aforementioned two fog droplet spectrometers, the laser holographic method (Liu and Liu, 1979) and opto-electronic method (Wang, 1981) are also used in China, which can be used to observe microphysical structures of fog.

b. Classification of fog types

Several approaches have been used in the classification of fog (Li, 2001; Gultepe et al., 2007; Niu et al., 2010b). Gultepe et al. (2007) summarized that the fog classification can be based on physical, thermo-dynamical properties, dynamical processes, chemical composition of particles, physiographic character of the surface, and meteorological features.

In the past studies of China, the fog are classified by the geographical location (sea (coastal) fog (Yang, 1985; Yang et al., 1989; Xu et al., 1994; Bao et al., 1995; Zhang and Bao, 2008; Huang et al., 2009; Koračin et al., 2014; Yue et al., 2014), inland fog (Li, 2001; Niu et al., 2010b; Fu et al., 2014)), terrain and human activities (mountain fog (Huang et al., 2000; Wu et al., 2007a; You et al., 2008), urban fog (Niu et al., 2010b; Li et al., 2011b, 2012)) (Fig. 1). Based on the fog process mechanisms, the fogs were also divided into advection fog, precipitation fog (The precipitation fog means the fog that appears during the process of light rain, in essence it is the evaporation fog caused by the evaporation of rain), radiation fog, and advection-radiation fog (Li, 2001; Gultepe et al., 2007; Niu et al., 2010b). Since many of the mountain fogs are influenced by human activities and urbanization (Jiang et al., 1994; Huang et al., 2001; Li et al., 2012), some researchers classified them into urban fog. Thus, the same fog process could be classified by different approaches.

In this review, we classify the fogs into urban fog, mountain fog and sea fog firstly (section 3a-3c, and section 3e), mainly based on the geographical location. The fog process mechanisms were also considered to analyze the unusual recent researches, so advection fog, precipitation fog, radiation fog, and advection-radiation fog would be discussed in section 3d, 3e and section 5. As the mountain fog could also be affected by human activities, the urbanization impacts would be discussed in section 4.

3. Fog microphysical structures

The observations of fog over the past 50 years have essentially revealed the fog microphysical characteristics in various places in China (Fig. 1). Table 1 lists these structures of mountain fog, urban fog and sea fog. We can see that the concentration of fog droplet is the largest in the city, and the order of magnitude is 10^2-10^3 per cm^3; it is smaller for sea fog, with an average order of magnitude of 10^1 per cm^3. Urban fog droplets are smallest, with average diameters mostly below 10 μm. The average diameters of fog in Shanghai and Chongqing are smaller than 5 μm. The size of sea fog in Zhoushan is the largest among sea fog, and its average diameter reaches 22.1 μm. The fog LWC in various locations is mostly in the range of 0.1-0.5 g m^{-3}. The fog LWC in Chongqing is the smallest, with an average of only 0.07 g m^{-3}.

a. Mountain fog

The earliest Chinese cloud-fog physics research started from mountain fog study and began in the late 1950s and early 1960s in Shanghai of China (Li, 2001; Niu et al., 2010b). A large-scale survey was carried out in southern China in later 1960s and 1980s, the observation sites including Yunnan, Guizhou, Sichuan, Chongqing, Guangdong, Fujian, Jiangxi, and Anhui provinces (Li, 2001; Niu et al., 2010b).

The mountain fogs have different microphysical features in the same site between different periods (it would be discussed in section 4), and there also have different microphysical structures between different sites as the human activities. The mountain fog influenced by the human activities would have larger fog droplets concentration, and small LWC (Li et al., 1992; Li and Peng, 1994; Huang et al., 2000; Tang et al., 2002). For example, Chengdu, Chongqing, Shuicheng and Loushan of Guizhou province are metropolises or industrial cities, they have the fog droplet concentrations mostly greater than 180 per cm^3, while the maximum are greater than 1000 per cm^3, and the maximum LWC are mostly lower than 0.5 g m^{-3}.

If human activities have less effect on the mountain fog, the concentration would be smaller, and the LWC would be larger. For example, Jianghong, Simao, Mengyang, Nanling Mountain, Tunxi, Yongan and Yongding, Lushan, are small cities/towns or mountain stations, they have the fog droplet concentrations mostly lower than 120 per cm^3, while the maximum are lower than 300 per cm^3, and the maximum LWC are mostly greater than 0.5 g m^{-3} (with the maxima LWC were

Table 1A. Microphysical structures of mountain fog in China (All of the instruments are the triplex droplet collector).

city	Date	site	Concentration (per cm^3)		LWC ($g\ m^{-3}$)		D_{ave} (μm)	
			Ave	Max	Ave	Max	Ave	Max
Chengdu, Sichuan (Li et al., 1992)	1970.12-1971.1	metropolis-suburban	256.4	285	0.17	0.34	10.3	31.7
	1985.12.15-1986.1.14		417.4	959	0.5	1.32	8.3	4.5
Chongqing (Yu and Su, 1990)	1987.11.20	metropolis	115	182	0.24	0.41	12.2	14.3
Shibanpo, Chongqing (Li and Peng, 1994)	1989-1990	metropolis-downtown	529	2026	0.03	0.16	4.4	7.5
Chenjiaping, Chongqing (Li and Peng, 1994)			453.8	1635.7	0.13	0.37	4.8	5.9
Shapingba, Chongqing (Li and Peng, 1994)			188	1436.6	0.18	0.48	9.4	16.4
Shapingba, Chongqing (Jiang et al., 2004)	2001.12	metropolis-suburban	1746.3	3072.2	0.21	0.5	3.8	5.2
Geleshan, Chongqing (Jiang et al., 2004)			983	2138	0.1	0.24	4.5	5.3
Loushan, Guizhou (Li et al., 1992)	1990	industrial city	267	1539	0.25	0.56	7.6	19.8
Shuicheng, Guizhou (Li et al., 1992)	1988.1989.1991		220	1178	0.16	0.47	7.2	14.3
Simao, Yunnan (Li et al., 1992)	1968-1969	small city	41.9	107	0.36	0.8	19.7	26.8
Jinghong, Yunnan (Li et al., 1992)			34.9	60.6	0.74	1.97	28.6	35
Jinghong, Yunnan (Li et al., 1992)	1986.12.26-1987.02.18		153	783	0.08	0.13	6.8	11.3
Mengyang, Yunnan			94.8	270.2	0.25	0.74	13.1	22.8
Menghai, Yunnan			48.5	111.9	0.21	0.75	15.4	26
Mengyang, Yunnan (Huang et al., 2000)	1997.11.26		81.7	38.5	0.04	0.12	9.2	27.2
	1997.11.28		313	955.2	0.04	0.19	7.3	17.6
	1997.11.29		315.2	2437.7	0.03	0.12	7.6	16.5
Tunxi, Anhui (Li et al., 1992)	1981.1		115.7	182.9	0.43	0.76	12.3	15.3
Yongan, Fujian (Li et al., 1992)	1968-1969		83.2	223	0.32	2.6	12.5	34.4
Yongding, Fujian (Li et al., 1992)	1968-1969		45.2	85	0.46	1.3	22.9	37.2
Nanling Mountain, Guangdong (Tang et al., 2002)	2001.02.24-02.28	mountain station	191.4		0.16		8.2	
	2001.03.07-08	mountain station	201.7		0.12		7.2	
	1999.1.11-1.15	mountain station	170.2		0.15		7.5	
	1999.1.18-20	mountain station	79		0.17		11.1	
	1998.12.31-1999.1.2	mountain station	47		0.1		13.3	
Lushan, Jiangxi (Li et al., 1992)	1981.1.11	mountain station	116	183	0.43	0.76	12.3	15.3

Table 1B. Microphysical structures of urban fog in China.

city	Date	Concentration (per cm^3)		LWC ($g\ m^{-3}$)		D_{ave} (μm)		instruments
		Ave	Max	Ave	Max	Ave	Max	
Xianghe, Beijing (Wang, 1981)	1978.11.5	160	172					Opto-electronic method
	1978.11.6	160	171					
	1978.11.7	167	188					
	1978.11.8	179	191					
Tianjin (Li Zihua, 2001)	1988.1				0.25			The triplex droplet collector
Shanghai (Gu, 1980)	1950S-60S		500	0.5	1.4			
Shanghai (Guo et al., 1990)	1989.1	173	518.4	0.26	1.53	9.9	5	
Tangshan, Jiangsu (Huang et al., 1998; Li et al., 1999)	1996.12.27	48.4		0.14		12.4		
Nanjing, Jiangsu (Huang et al., 1998; Li et al., 1999)	1996.12.29	152.6		0.09		6		
	1996.12.29	1517		0.17		4.6		
	1996.12.30	2047.7		0.25		4.5		
Yangcheng lake, Jiangsu (Huang et al., 1998)	1997.1.21	268.6		0.04		4.8		
Wuxue, Hubei (Yu and Su, 1990)	1987.11.20	124	201	0.68	1.3	11.7	14	
Chenglingji, Hunan (Yu and Su, 1990)	1987.11.21	121	159	0.67	1.24	12.3	15.8	

Table 1C. Microphysical structures of sea fog in China.

Site	Date	Concentration (per cm^3)		LWC ($g\ m^{-3}$)		D_{ave} (μm)		D_{max} (μm)		instruments
		Ave	Max	Ave	Max	Ave	Max	Ave	Max	
Shanghai (Bao et al., 1995)	1989.1	198	939	0.18	1.27	4.7		59.5	137	The triplex droplet collector
Qingdao, Shandong (Yang, 1985)	1980.5.3	100.2		0.06		48.0				
	1980.5.13	100.0		0.04	0.076	48.0				
Zhoushan, Zhejiang (Yang et al., 1989)	1985.4.21-22	43.1	72.5	0.15	0.50	24.1		50.9	88.9	
	1985.5.6	53.5	109.3	0.08	0.25	17.8		55.9	181.6	
	1985.05.9-10	29.0	87.3	0.10	0.23	21.1		62.0	145.1	
	1985.5.12	2.2	48.1	0.09	0.27	27.7		84.4	338.1	
	1985.5.18	36.3	65.9	0.11	0.22	18.9		51.6	104.1	
	1985.5.19	35.6	122.0	0.13	0.39	22.9		53.0	93.4	
	1985.4-5	37.1	122.0	0.37	2.68	22.1	27.7	59.6	338.1	
Qingdao, Shandong (Xu et al., 1994)	1993.6.29-7.2	82.46	248.9	0.07	0.19	4.5	5.0			
Bohe, Guangdong (Huang et al., 2009)	2007.3.24-25	56.30		0.04		5.2				
	2007.3-4	57.10	111.9	0.02	0.18	4.7	15.3	25.4	56.1	
Zhanjiang, Guangdong (Yue et al., 2013, 2014)	2010.3.24-25	57	402	0.02	0.21	4.6	26	26.8	49.0	The laser backscattering fog droplet spectrometer
	2011.3.20-21	231	616	0.11	0.59	6.6	13.6	36.8	49.0	

Table 2. Characteristics of microphysical structures for four types of fog in Nanjing during 2006-2009 (Niu et al., 2012).

Fog types		visibility	Wind speed	Temperature	RH	Concentration	LWC	D_{max}	D_{ave}	instruments
	unit	m	m s^{-1}	ºC	%	per cm^3	g m^{-3}	μm	μm	
radiation fog	Ave	385	0.6	4	99.8	77.9	0.023	12.69	3.66	The laser backscattering fog droplet spectrometer
	Max	1000	5.2	14.1	100	993.2	0.48	50	8.56	
	Min	15	0	–1.1	88.3	1	0.01	4	3	
precipitation fog	Ave	605	1.3	7.4	99.3	2.5	0.04	5.09	3.05	
	Max	1000	5.7	11.3	100	12.3	0.21	8	3.34	
	Min	214	0	5	84.3	1	0.01	0	0	
advection fog	Ave	292	1.2	6.2	97.6	107.8	0.021	17.39	3.59	
	Max	1000	3.9	9.7	100	1914.7	0.98	48	5.53	
	Min	50	0	2.9	86	1	0.01	4	3	
advection-radiation fog	Ave	191	0.7	3.8	99.1	211	0.12	27.13	4.99	
	Max	1000	5.3	8.6	100	1213.8	0.90	50	9.47	
	Min	15	0	–0.2	85.5	1	0.01	4	3	

2.6 g m^{-3} in Yongan and 1.3 g m^{-3} in Yongning, respectively) (Li et al., 1992).

b. Urban fog

Before 2000, inland urban fog microphysics observations used the triplex droplet collector. Nanjing had the largest fog concentration in all urban cities, not only befroe 2000 (Table 1B), but after 2006 (Table 2), these were mostly greater than 1000 per cm^3 (Huang et al., 1998; Li et al., 1999; Li et al., 2011b; Niu et al., 2012), and the fog concentrations in Beijing (Wang, 1981), Tianjin (Li, 2001), Shanghai (Gu, 1980; Guo et al., 1990) were all about 160-180 per cm^3; these are similar with that of some mountain fogs of Chengdu, Chongqing, Shuicheng and Loushan of Guizhou province mentioned in section 3.1.

Wuxue of Hubei Province and Chenglingji of Hunan Province (Yu and Su, 1990) had lower fog concentrations, which were 120 per cm^3 or so. However, Wuxue of Hubei Province, Chenglingji of Hunan Province and Shanghai had fog LWC greater than 1.0 g m^{-3}, similar with some mountain fogs of Jianghong, Simao, Mengyang, Nanling Mountain, Tunxi, Yongan and Yongding, Lushan, mentioned in section 3.1, much higher than those of Beijing and Tianjin, which may be related to the water vapor differences between north and south areas.

The differences between these urban fogs and human activities affected mountain fog concentrations and LWC maybe led by the different aerosol pollution levels in various cities and period. Ding and Liu (2014) analyzed that the fog days in China had an increasing trend before 1980 and a decreasing trend after 1990, but the number of haze days has demonstrated an increasing trend. The aerosol concentrations increase maybe the primary factor.

The fog microphysics are greatly influenced by urbanization, as will be described in Section 4.

c. Sea fog

The earliest Chinese sea fog microphysics research started in 1980 in Qingdao (Yang, 1985), the fog droplet concentrations were about 100 per cm^3, and the maximum fog LWC was 0.076 g m^{-3}.

There were several sea fog observations between 1980 and 2000 (Yang et al., 1989; Xu et al., 1994; Bao et al., 1995). In these fog cases, there were more than 5 cases that the maximum water content was more than 1 g m^{-3}, and the maximum sea fog LWC was 2.68 g m^{-3} (Yang et al., 1989);

After 2005, sea fog observations were carried out along the coast of northern South China Sea in Guangdong Province (Bohe, Huang et al., 2009; Zhanjiang, Yue et al., 2013, 2014). The South China Sea fog concentrations were about 100-400 per cm^3, and the maximum fog LWC was 0.18 g m^{-3}.

From the above analysis, sea fog has the largest LWC, this special results may be led by different observation instrument. The triplex droplet collector measurement scale ranges from 3.2 to 70 μm, but the laser backscattering fog droplet spectrometer particle size range is 2-50 μm.

d. Differences in fog microphysical characteristics

Further studies indicated that microphysical structures varied in different types of fog. Table 2 gives the characteristics of microphysical structures for four types of fog obtained during the fog observations in winters of 2006-2009 in Nanjing (Lu et al., 2008, 2010b; Li et al., 2011a, 2011b; Liu, 2011; Liu et al., 2011, 2012a, 2012b; Niu et al., 2010a, 2012). We can see that the concentration of fog droplets is the largest for advection-radiation fog, with an average of 211.0 per cm^3; it is followed by advection fog and radiation fog, with averages of 107.8 and

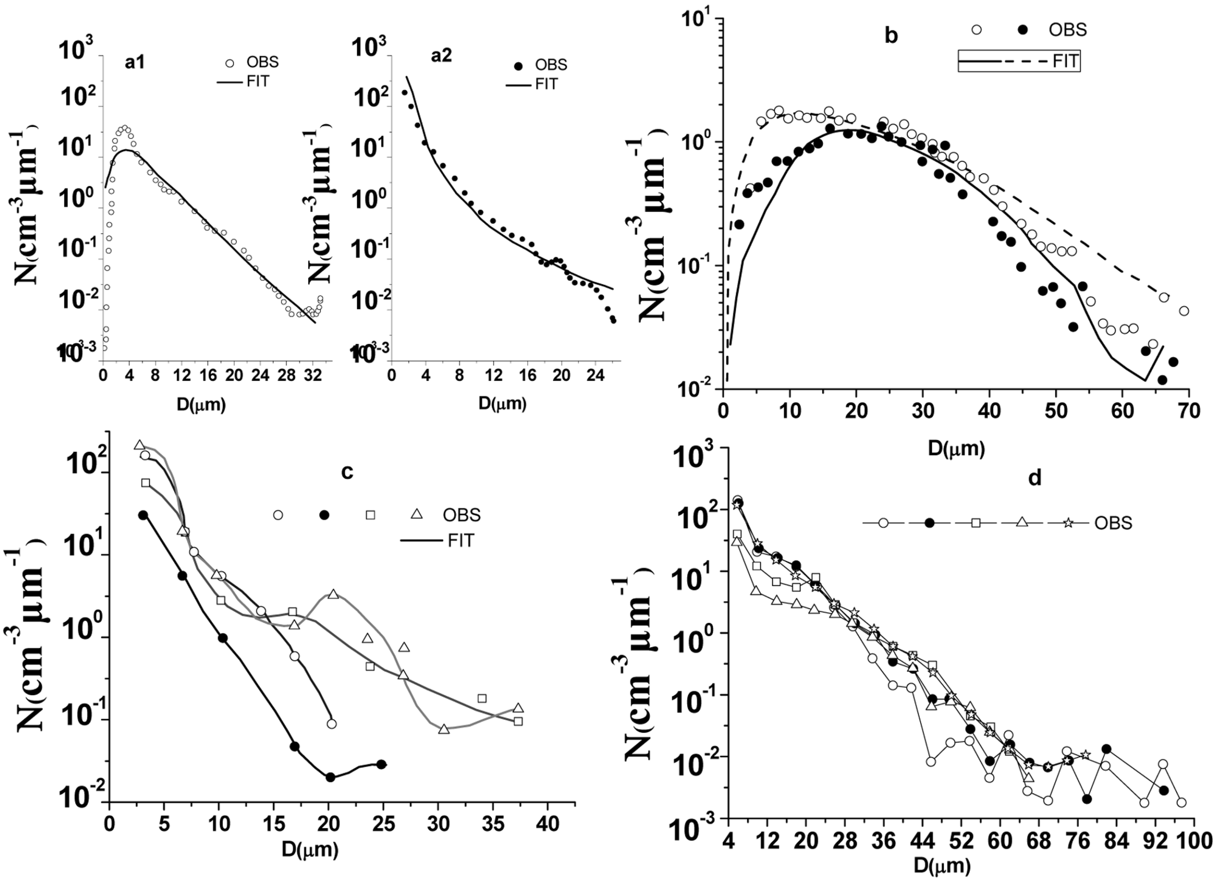

Fig. 2. Fog droplet spectral distributions of urban fog (a_1: Shapingba of Chongqing; a_2: Chenjiaping of Chongqing, (Li and Wu, 1995) (○● are the observed data, solid line is the fitting curve)), sea fog (b: Zhoushan of Zhejiang (Yang et al., 1989) (○: mainland direction observed values, ●: sea direction observed values, dotted line is the mainland direction fitting curve, solid line is the sea direction fitting curve), c: Qingdao (Xu et al., 1994) (○●□△: observed values, lines are the fitting curves)), and mountain fog (d: Nanling Mountain, observed values, Deng et al., 2007b)) in China.

77.9 per cm^3, respectively; the concentration of fog droplets is the smallest for precipitation fog, only 2.5 per cm^3. The LWC is also the largest for advection-radiation fog, with an average of 0.12 g m^{-3}, followed by LWC of advection fog and radiation fog, with averaged values of 0.02 and 0.023 g m^{-3}, respectively; the LWC of precipitation fog is the smallest, with a maximum of only 0.21 g m^{-3}. The average diameter of advection-radiation fog is the largest, at 4.99 μm; it is 3.66 μm for radiation fog, 3.59 μm for advection fog, and only 3.05 μm for precipitation fog. The largest droplet of precipitation fog is only 8 μm, whereas it can reach 50 μm for other types of fog.

e. Characteristics of droplet spectral distribution

The characteristics of fog droplet spectral distribution are an important aspect of microphysical features of fog. Figure 2 shows the features of spectral distribution for typical urban, sea and mountain fogs. We can see that the fog droplet spectrum of sea fog is relatively wide, and the most common diameter is relatively large (10-20 μm), while the dN/dlogD value is relatively small.

The sea fog spectral distribution in Zhoushan (Yang et al., 1989) areas are all satisfies the Deirmenjian distribution, both the mainland direction ($N(D) = 0.3214D^{1.157}\exp(-0.1052D^{0.95})$) and the sea direction ($N(D) = 0.001269D^{3.524}\exp(-0.1855D)$). While all the sea fog spectral distribution in Qingdao are more consistent with the Junge distribution ($N(D) = 786D^{-5.2}$).

The most common diameter for fogs in Chongqing is very small (< 4 μm), and the largest diameter in Chongqing is also very small (generally < 35 μm). The spectra are different at different sites in the city. The spectral distribution in Shapingba of a suburban areas satisfies the Deirmenjian distribution ($N(D) = 17797D^{5.21}\exp(-0.8.21D^{0.4})$), while the spectral distribution in Chenjiaping of an urban area is more consistent with the Junge distribution ($N(D) = 2590D^{-3.4}$). In Chenjiaping, the concentration of small droplets is large, and the droplets smaller than 2 μm account for 80% of the number of fog droplets, whereas it only accounts for 32% in Shapingba. The fog droplet spectrum in Chenjiaping is very narrow, with a spectral width of 26 μm, whereas the spectral width in Shapingba is 33 μm. The five spectral distributions for mountain fogs in Nanling indicate that the fogs are dominated by

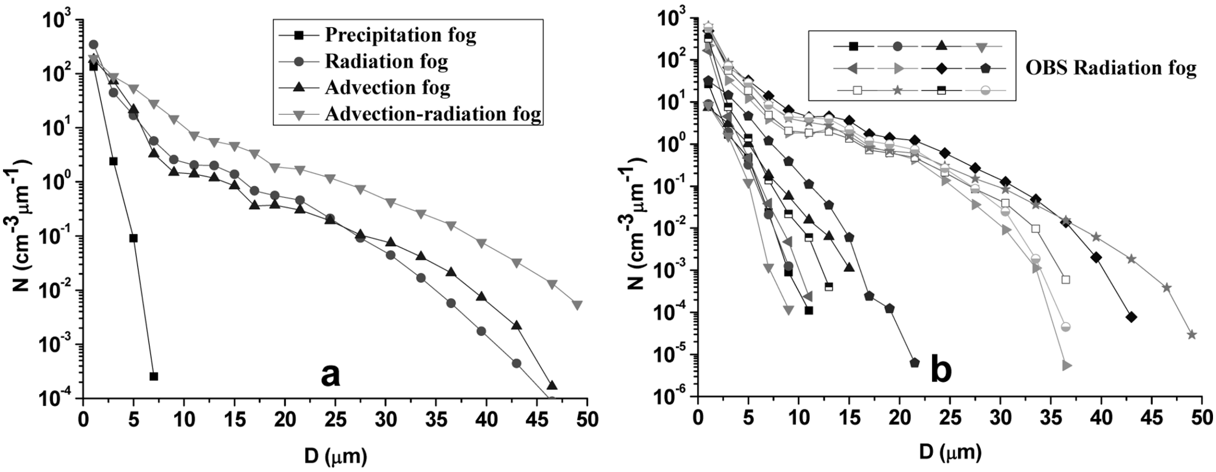

Fig. 3. Averaged droplet spectral distributions of four types of fog (a) and of all radiation fogs (b) in Nanjing (Drop number size distribution in the form of dN/dlogD (cm^{-3}μm^{-1})). Source from Niu et al. (2012).

small droplets, mostly with diameter < 16 μm; the fogs in the large droplet segment exhibit a significant multi-peak ripple feature.

The observations of fog in Nanjing indicate that the spectral distribution varies for different types of fog. Figure 3a shows the average spectral distribution characteristics for four types of fog (Niu et al., 2012). We can see that the spectral distribution of precipitation fog (also called evaporation fog) is relatively narrow, and the largest droplet is no more than 7 μm. The spectrum of advection radiation fog is the widest, and its curve is similar to that of other types of fog. The spectral distributions of radiation fog and advection fog are similar, with relatively small differences, but for the spectral segment greater than (or less than) 24 μm, N value of radiation fog is smaller than (or greater than) N value of advection fog. The spectral distribution of each radiation fog is also unique. The observations indicate that the radiation fog in Nanjing has two spectral distribution features. One type of spectral distribution is relatively wide, exhibiting a convex shape, and the largest spectral width exceeds 35 μm, which is called wide-spectrum radiation fog. The other type of spectrum is relatively narrow, with a spectral width mostly no more than 15 μm, and only reached 23 μm in one fog process, which is called narrow-spectrum radiation fog (Fig. 3b) (Niu et al., 2012). Generally speaking, wide-spectrum radiation fog is extremely dense fog (visibility < 50 m), and narrow-spectrum radiation fog is dense fog (visibility < 500 m). The spectral widening of the wide-spectrum radiation fog will be detailed analyze in section 5.

The wide and narrow radiation fogs in Nanjing are unique in four types of fogs. From the mean size distributions we can see that the advection radiation fog and advection fog spectrums are all wider than that of radiation fog. The narrow spectra may be owing to the fact that these radiation fogs did not go through outbreak growth, the feature of which would be further discussed in section 4.

The differences of the number concentrations, LWC, and droplet size distributions (DSD) between these different urban fog types may be impacted by the fog boundary layer features, the inversion intensity, humidity conditions, wind speed, etc., which could influence the aerosol activation, condensation growth, coalescence growth, leading to the different micro-physical features and droplet spectral distribution (Yang et al., 2010a; Liu et al., 2011, 2012a).

4. Impacts of urbanization on microphysical structures of fog

The observations indicate that the microphysical structures of fog at different urban sites are also different. Table 1A lists the average values and variation ranges for the main micro-physical parameters observed at different sites in Chongqing from 15 December 1989 to 15 January 1990 (Li and Peng, 1994). We can see that from downtown Shibanpo to Shapingba in the suburban, the concentration of fog droplets became smaller, and the size of fog droplets and LWC became larger. In the downtown area, the average concentration exceeded 500 per cm^3, whereas the average diameter was only 4.4 μm, and the LWC was less than 0.1 g m^{-3}. In comparison, for Shapingba in the suburban, the concentration was twice as large, the average diameter was half, and the LWC was smaller by a factor of five. These micro-structure distributions were related to the urban heat island effect and the distribution of aerosol particles. The observations indicate that the heat island effect was significant in the urban area of Chongqing. From the city center to the suburban area, the temperature gradually declined, and the downtown temperature at night was at least 2°C higher than that in the suburban (Li et al., 2012). Because the temperature in Shapingba was low, the saturation temperature of water vapor was high, the condensation growth of fog droplets was large, and the fog LWC was high. In the central city, the intensity of the heat island was high, which means that the cooling of air was not strong enough for the saturation

Table 3. Microphysical parameters of two types of radiation fog (Li et al., 2011a).

	wide-spectrum radiation fog		narrow-spectrum radiation fog		instruments
	average	range	average	range	
Concentration (/cm^{-3})	121	1-1213	12	1-723	
LWC (g m^{-3})	0.039	$1.82{\cdot}10^{-5}$-0.479	0.00056	$5.47 \times 10^{-6} \sim 0.059$	
D_{ave} (μm)	3.98	3-8.60	3.20	3-4.67	The laser backscattering fog droplet spectrometer
D_{peak} (μm)	3.0	3.0	3.0	3.0	
D_{max} (μm)	16.12	2.0-50	6.7	4.0-23.0	
samples	30434		12724		

level of air to be high for fog formation. The fog droplets could undergo condensation growth, and therefore, the fog droplets were small and the LWC was low. In the urban area of Chongqing, air pollution was severe, and the concentration of aerosol particles in the air was very high. Observations using the LG-83 multi-channel optical particle counter indicated that the maximal concentration was located in the city center, and its value was about twice the levels in the suburbs and outskirts. Because there were many aerosol particles in the city center, there were many atmospheric condensation nuclei, and therefore the concentration of fog droplets was high. In general, if the water vapor content in the air is fixed, the larger the concentration of fog droplets, the smaller the size of the fog droplets (Li et al., 2012).

By comparing observation data over different periods in the same area, we can see the impacts of urbanization on microphysical structures of fog. Table 1A lists the results of several observations in Jinghong, Yunnan Province (Li et al., 1992). These observations used the same apparatus (triplex droplet collector). In 1968-1969 (Table 1A), the LWC of fog in Jinghong was 0.74 g m^{-3}, with an average diameter of 28.6 μm and a concentration of only 34.9 per cm^3; however, during the observations in 1986-1987, the average LWC was only 0.08 g m^{-3}, and the average diameter was 6.8 μm, while the concentration increased to 153 per cm^3. In less than 20 years, the LWC of fog decreased by nearly one order of magnitude, while the concentration increased nearly five times. On 23-30 November 1997, another observation of fog droplet spectrum was conducted in Jinghong. Although there were four episodes of fog during this period, it was difficult for the triplex droplet collector to take samples. We only used the absorbent paper mark method to measure the LWC. The results (Huang et al., 2000) indicate that the maximum LWC was 0.061 g m^{-3}, and the minimum was only 0.008 g m^{-3}, which was significantly less than that during the winter in 1986. The variation in fog deposition amount recorded at Jinghong weather station also indicated a downward trend of LWC in fog. In the 1950s, the average annual total amount of fog deposition was 17.3 mm; it decreased to 4.4 mm in the 1970s and it was less than 1 mm in the 1980s. After that, it became difficult to collect fog data, and the fog deposition was very small (Li et al., 2012). The variation in the microphysical structures of fog in Xishuangbanna was directly related to urbanization and global warming. Early in the post-liberation period (starting in 1949), the forests were dense. This area was sparsely populated, and the population of Jinghong was approximately 1000, with only six tile-roofed houses. The population of Jinghong reached hundreds of thousands year by year, and there were many tall buildings in the urban area, which expanded to dozens of square kilometers. There were hundreds of enterprises and 57,000 vehicles. All of these factors directly contributed to the urban heat island effect. Meanwhile, the global warming maybe the factor leading the fog microphysical features variation. Ding and Liu (2014) analyzed that the number of fog days of the surface weather stations in China has a decreasing trend after 1990, which is consistent with the decreasing trend of the surface relative humidity.

The fog day in Jinghong dropped from 166 days during 1954-1959 to 58 days during 1990-1995 (Gong and Ling, 1996). And the temperatures in Jinghong has gradually increased from 21.4°C in 1960s to 22.7°C during 1990-1995. In comparison with the 1960s, the annual average temperature increased by approximately 1°C. Urbanization also caused the humidity to decrease. As for the relative humidity at 20 local times during the winter half of the year (fog season), which was directly related to the formation of fog, it decreased rapidly from 85% in the 1950s to 71% and 73% in the 1980s and 1990s, declining by 12% and 14%, respectively. One important cause of the variation in the microphysical structures of fog in Xishuangbanna was the decrease in green land and decline in the forest coverage rate. Xishuangbanna used to be a famous tropical rainforest foggy area in China. Due to urban development, the tropical rainforest and foggy days are decreasing every year (Gong and Ling, 1996).

5. Macroscopic conditions and microphysical processes for the spectral widening of radiation fog droplets

As mentioned in Section 3, the radiation fog in Nanjing has two features of spectral distribution. In general, the wide-spectrum radiation fog is extremely dense fog (visibility < 50 m), and the narrow-spectrum radiation fog is dense fog (visibility < 500 m). Table 3 gives the average microphysical

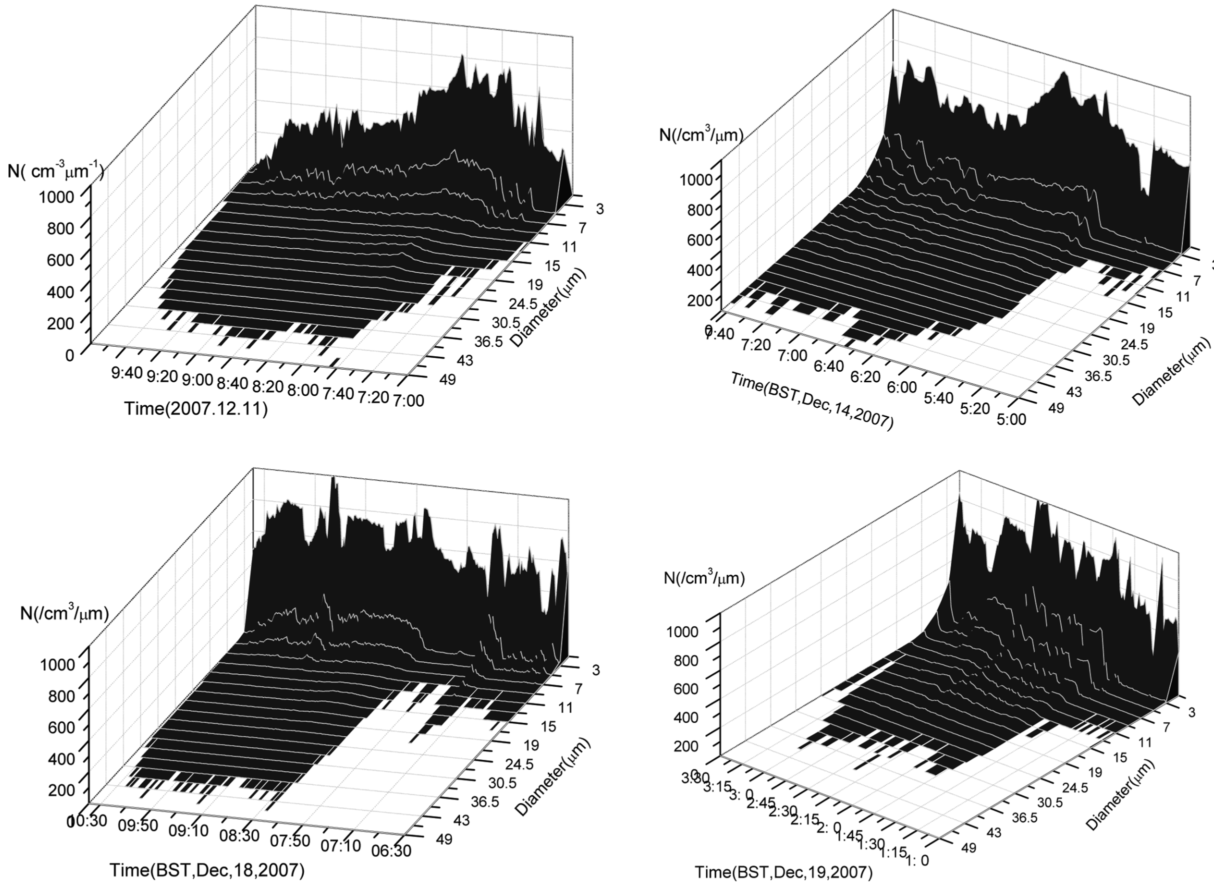

Fig. 4. Time evolutions of radiation fog and advection-related fog droplet spectra in Nanjing. Source from Li et al. (2011a).

parameters of 13 radiation fog cases for the entire life cycles from generation to dissipation of these two types of radiation fog (6 wide-spectrum radiation fog cases and 7 narrow-spectrum radiation fog cases).

As shown in the table, the concentration of fog droplets for the wide-spectrum radiation fog is larger than the concentration for the narrow-spectrum radiation fog by one order of magnitude, and the LWC for the former is larger by two orders of magnitude. The biggest difference is the spectral width: the width of wide-spectrum radiation fog is twice as large as that of narrow-spectrum radiation fog.

The widening of fog droplet spectrum is generally characterized by an outbreak feature (Fig. 4); that is, in a very short time interval (approximately 30 min), the concentration of fog droplets increases by approximately one order of magnitude. The spectral width of fog droplet spectrum exceeds 20 μm and can generally reach 30-40 μm or even 50 μm. The result is that the LWC increases significantly (generally by two to three orders of magnitude). The visibility distance decreases to < 50 m, and the dense fog changes rapidly to extremely dense fog. The outbreak feature of fog droplet spectral broadening has been found many times in Nanjing, and it requires further observation and study to determine whether the development of extremely dense fog in other places also involves this widening.

The common feature of the mentioned several fog types is the significant cooling or humidifying in the surface fog layer upon outbreak. The air in the fog body has been saturated. During cooling and humidification, it will increase the saturation. Therefore, the burst broadening of fog droplet spectrum actually occurs under the condition of enhanced saturation.

Under what type of macroscopic condition does the broadening of fog droplet spectrum occur? The analysis of several fog cases in Nanjing indicated that on days of dense fog, the wind turned to a cold northerly wind, and wind speed was less than 1 m s^{-1}. That is to say when there is weak cold advection, it will cause the development of fog outbreak. After sunrise, the ground evaporation enhances, which not only decreases temperature but also increases water vapor in the dense fog area and therefore contributes to the burst enhancement of fog body. At night, the longwave radiation is enhanced, and the temperature drops dramatically to contribute to the burst broadening of fog droplet spectrum. In addition, the upper-layer warm advection in the fog area, the cold advection in the ground layer, and the turbulent mixing effect can also cause burst development in the fog area.

How does the fog droplet spectrum broaden in an outbreak? What are the microphysical processes? Along with the en-

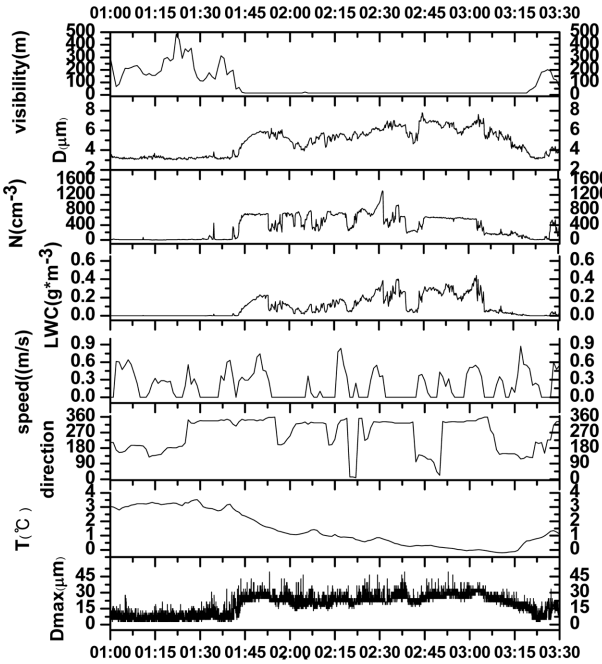

Fig. 5. Temporal variation of microphysical parameters of extremely dense fog on 19 Dec 2007: 0100-0330 BST. Source from Li et al. (2011a).

hancement of temporal resolution of fog droplet spectrum observation, it is now possible to discuss these questions by analyzing the continuous variation of fog droplet spectrum over each minute and second. In general, the widening is step by step. Before each widening, the curve of the fog droplet spectrum is significantly elevated, namely, the concentration of each range increases. Individual large droplets appear to the right side of curve and then the curve broaden to the large droplets. After a few minutes, when fog droplet spectrum is relatively flat or undulates, the curve of the fog droplet spectrum is again lifted and broadened until 40-50 μm. During the early stage of broadening, nucleation and condensation dominate, and all sizes of fog droplets increase rapidly. Subsequently, the fog droplet spectrum broadens to 20 μm. In the middle of broadening, there are nucleation and collision processes. First, the fog droplets larger than 10 μm increase significantly, and then large droplets of approximately 30 μm appear; late in the broadening, a similar collision process again appears, which broadens the fog droplet spectrum to above 40 μm. When the cooling rate is very large and the over-saturation is significant, the broadening rate of the fog droplet spectrum is also very large, and there are essentially no aforementioned "steps": the spectral width continuously increases, and the number of fog droplets on various levels keeps increasing. After 01:40 on 19 December 2007, the temperature declined at the rate of 1.5°C 12 min^{-1}; after 01:41, the curve of the spectral distribution was constantly elevated, and the spectral width continued increasing; at 01:47, the largest droplet increased from 10 to 30 μm. After seven minutes, the spectral width increased by 20 μm (Fig. 5). The numbers of fog droplets on various levels increased, which increased the concentration of fog droplets by a factor of more than 50, and the LWC increased by three orders of magnitude. These observations indicate that not only the collision process but also the nucleation and condensation processes proceeded quickly.

From the 6 wide-spectrum radiation fog cases, it indicated that during the widening process of fog droplet spectrum, the variation of turbulent intensity was synchronized. Turbulent diffusion plays a significant role in the vertical transports of momentum, heat and water vapor (the ultrasonic anemometer was used during the observation, Li et al., 2011a). After the turbulent intensity reached the peak, sensible heat flux changed from negative to positive value, and the ground heat transfer upwards. At the same time, the upward transportation of water vapor also reached the peak value, and transported upward through the turbulent diffusion. The transportation created great conditions for the fog droplets spectral explosive broaden. Meanwhile, the turbulent collision is an important mechanism for the growth of large droplets (Li et al., 2011a).

The study of the burst broadening of fog droplet spectrum is of significant practical application because a variety of major traffic accidents tend to occur in extremely dense fogs, especially when the dense fog suddenly intensifies into extremely dense fog. It also has a certain theoretical significance in the field of cloud and fog physics because in the study of the warm cloud precipitation mechanism, how the large droplets in the cloud are formed is always a scientific question of primary interest.

6. Microphysical features in the fog-haze conversion

Fog is the aggregate of a large number of water or ice particles suspended in the near-surface air and can reduce the horizontal visibility to below 1 km. Haze is the aggregate of a number of tiny dust particles, soot, or salt particles suspended in the air that makes air muddy and reduces the horizontal visibility to below 10 km. We can see that fog and haze are two weather phenomena of entirely different concepts. Currently, we often link them together and call them 'fog haze'. This conflation occurs because they both affect the visibility (distance) and both are harmful to human health. Moreover, they can be transformed into each other under certain condition. When the air humidity reaches saturation, haze particles can transform to fog droplets; when the relative humidity decreases, the fog droplets can evaporate to leave haze particles. Yang et al. (2010b) studied the continuous fog-haze process in Nanjing during 15-29 December 2007. They divided the entire process into four different stages of fog, mist, wet haze, and haze. According to the magnitude of LWC and horizontal visibility (distance), they called the particle groups dominated by water droplets fog and mist, and called the aerosol particle groups composed of non-water droplets haze and wet haze. The specific criteria for classification are listed in Table 4. According to the table, the weather

Table 4. Criteria of weather classification and data summary (Yang et al., 2010b, 2012).

Weather	Fog	Wet Haze	Haze	Mist
Visibility (m)	< 1000	< 1000	1000-10000	1000-10000
LWC (g m^{-3})	$\geq 1.0 \times 10^{-4}$	$< 1.0 \times 10^{-4}$	$< 1.0 \times 10^{-5}$	$\geq 1.0 \times 10^{-5}$
RH (%)	95.3	91.0	79.1	79.3
Sample	4283	2301	3135	5698

phenomenon with visibility < 1000 m and LWC greater than or equal to 1.0×10^{-4} g m^{-3} referred to as fog, while the one with lower values is called wet haze, and the threshold of LWC for haze or mist is 1.0×10^{-5} g m^{-3} because when LWC is below this value, the measured concentration of particles larger than 2.5 μm is smaller than 1 cm^{-3}. Table 4 also gives the average relatively humidity for four types of weather phenomena: > 95% in the fog state, > 90% in the wet haze stage, and approximately 80% in the haze and mist stages.

Through continuous observation using an FM-100 fog droplet spectrometer, the spectral distribution for the size of coarse particles with size > 2 μm (including fog droplets and non-liquid water particles) was derived (Fig. 6). We can see that the particle spectrum in the fog state is significantly wider than that in the other three stages. The largest diameter reached 40-50 μm and was dominated by fog droplets. On the spectral distribution curve of the surface area concentration and volume concentration, there are peaks at 5, 13 and 21.5 μm. The stages of mist, wet haze and haze are clearly different from the fog stage and all have single peak. The high-concentration particles are located on the side of small droplets, and the particles with size > 10 μm are only present in a small amount at the wet haze stage. These observations indicate that these three stages are dominated by micrometer-scale (hygroscopic) aerosol particles. The number concentration, surface area concentration and volume concentration of coarse particles of various sizes in the fog stage are significantly larger than those in the other three stages. In particular, the number concentration is the lowest in the haze stage. By comparing the spectral distribution curves for the number concentration of mist and wet haze, we can see a boundary at 4 μm: the particles with size < 4 μm are more at the mist stage than at the wet haze stage, whereas the opposite holds for > 4 μm. This result indicates that during the transformation from mist to wet haze, as the relative humidity increases, certain particles with size < 4 μm in the mist stage absorb water and enlarge to become particles with size > 4 μm in the wet haze stage, increasing the concentration of particles > 4 μm in the wet haze stage. However, when the particles become larger, the coalescence and deposition processes become stronger. Therefore, relatively speaking, the concentration of particles with size < 4 μm decreases considerably in the wet haze stage, whereas the concentration of particles with size > 4 μm increases only moderately.

From the perspective of the distribution curves of surface area spectrum and volume spectrum, the contribution of fog droplets of < 25 μm to the surface area is the largest, and the contribution of fog droplets of 10-30 μm to the volume and LWC is the largest. The volumetric distributions of wet haze, mist and haze indicate that the particles near 3 μm make a significant contribution, whereas peaks are not formed after this size.

According to the analysis above, for the spectral distributions of coarse particles under four types of weather conditions, the spectral shapes exhibit the feature of gradual transformation from haze, mist and wet haze to the fog stage, which corresponds to the transformation process of "haze-mist-wet haze-fog-wet haze-mist-haze" during the observation period.

Figure 7 (Niu et al., 2012) shows the spectral distributions of the number concentration of fine particles (0.010-2.000 μm), measured by the wide-range particle size spectrometer under four different weather conditions. We can see that the characteristics of aerosol spectral distribution at the stages of fog, wet haze, mist, and haze exhibit clear features. The spectral shapes of the number concentration for fine particles in the stages of mist and haze are similar, and the number concentration in the stage of mist is the highest. The peak number concentrations in the stages of fog and wet haze are comparable, whereas the peak diameter in the fog stage is larger than that in the wet

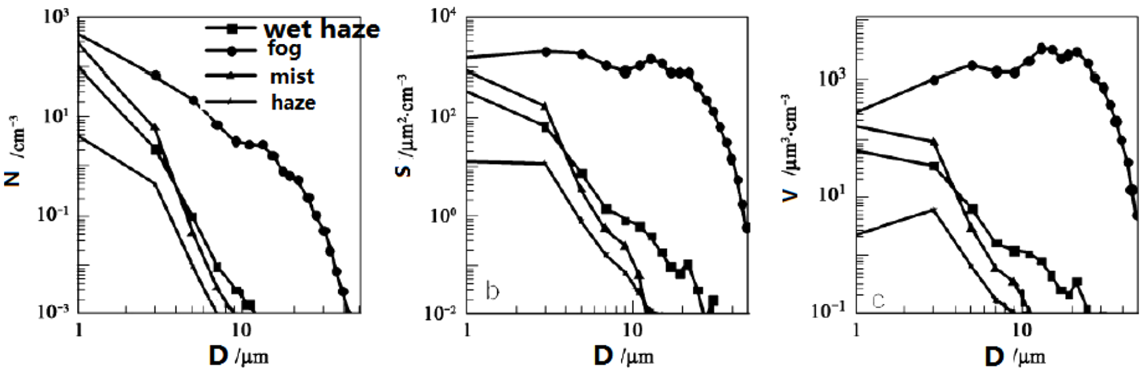

Fig. 6. Size distributions of coarse particle number, surface area and volume concentration in four weather conditions. Source from Yang et al. (2010b).

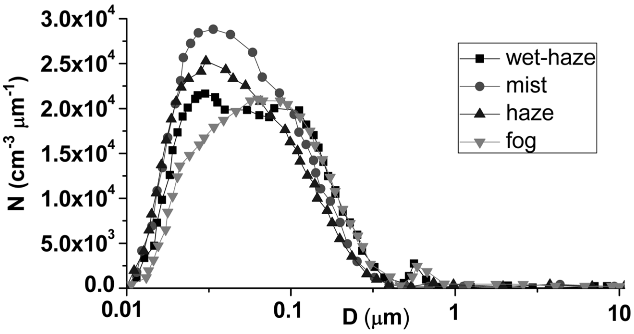

Fig. 7. Size distributions of fine particle number and surface area concentration in four weather conditions. Source from Niu et al. (2012).

haze stage.

For the four stages, the largest difference in the number concentration of fine particles appears in the range of 0.020-0.060 μm and is ordered from high to low for mist, haze, wet haze, and fog. In the fog stage, the number concentration of particles of 0.04-0.13 μm accounts for 51% of the concentration of total aerosol particles. The range of dominant particles in the wet haze stage is the widest, and the particles of 0.02-0.14 μm account for 75% of the total concentration. The size ranges of dominant particles in the stages of mist and haze are comparable (0.02-0.06 μm), and the sum of both accounts for 52% of the number concentration of total particles.

The calculations of Pandis et al. (1992) indicated that short-duration fog is not sufficient to remove most aerosol particles from the atmosphere through the wet elimination process of fog droplets. As fog dissipates, the fog droplets that experience heterogeneous chemical reaction evaporate to form new aerosol particles. These newly generated aerosol particles often have strong hygroscopicity and will generate haze when the concentration is relatively high (Pandis et al., 1992).

Yang et al. (2012) found that the dense fog process is a source of aerosol particles. The gas and liquid chemical reactions can contribute to the generation of new aerosol particles in the atmosphere. When the fog dissipates, the fog droplets evaporate, and the content of aerosol particles in the air could be larger than that before the fog. However, it is also a sink of aerosol particles. The wet elimination effect of fog droplets removes aerosol particles from the atmosphere, and the PM_{10} concentration reaches the minimum late in the stage of extremely dense fog. In the stage of extremely dense fog, the removal by fog droplets of the aerosol particles intensifies through the processes of aerosol activation, collision and adhesion. In the dissipation stage of fog, the PM_{10} concentration is higher than that in the development stage.

Studies on the fog-haze transformation are limited, and the aforementioned study is preliminary. As we pay more attention to this problem, we believe that in the near future there will be numerous studies on this subject in China, and the understanding of this problem will be greatly improved.

7. Other studies on microphysics of fog

a. Studies of extinction features of fog droplet

Fog can affect visibility because of the light extinction effect of fog droplets. Fog droplets affect the propagation of light through absorption and scattering, and therefore affect visibility. According to the visibility formula $R = (1/\beta_{se})\ln(1/\varepsilon)$ (Sheng et al., 2003), where the coefficient of light extinction is $\beta_{se} = (3/2)(L_w/\rho r_e)$, many empirical formulas were obtained. Let the threshold contrast of observers be $\varepsilon = 0.02$ and let water density be $\rho = 1$, the visibility formula becomes $R = 2.61(r_e/L_w)$, where r_e is the effective radius of fog droplets. The length unit used by visibility R should be the same as r_e and is the same as the length unit used to calculate LWC, which is usually meters. The equation above is called Trabert's Law.

Many studies were conducted in China on relationships between visibility in fog and microphysical parameters. Yang (1985) studied the sea fog near the coast of Qingdao and derived a simplified equation relating visibility and LWC, $R = 0.027 \bullet W^{-0.72}$, where R is visibility and W is LWC. Xu et al. (1994) derived $R = 5.74/W$; Huang et al. (2009) studied the sea fog near the northern coast of the South China Sea and derived $R = 0.085 \bullet W^{-0.61}$.

The above equations concern the relationship between R and W. According to Trabert's Law, not only the LWC but also the size of fog droplets can affect visibility. When LWC is fixed, the smaller the fog droplets size (when the concentration of fog droplets is larger), the smaller the visibility. The observations of city fog in different years indicated that, with the development of cities, the concentration of fog droplets became larger, while the size of fog droplets and LWC became smaller. Therefore, the visibility in fog was reduced. Consequently, in the study of visibility in fog, the size and concentration of fog droplets must be considered.

The coefficient of light extinction in fog changes with wavelength. Li et al. (2009) compared the observation data in Beijing and found that when the wavelength was smaller than 2.4 μm, the extinction coefficient of ground fog was higher than that of fog at the top of mountains. As the wavelength increased, the extinction coefficient of fog aerosols decreased. There are minimum values for the extinction coefficient near the wavelengths of 3.0, 5.0 and 11 μm, respectively. When the wavelength is greater than 11 μm, the extinction coefficient begins to increase, reaches a maximum at approximately 15 μm, and then begins to decline.

In the study on the extinction of atmospheric aerosols during sea fogs, Sheng et al. (2011) found that the average extinction coefficient of aerosol particles during fogs was 1.21 km^{-1}. In particular, the average extinction coefficient of condensed particles smaller than 0.5 μm was 0.55 km^{-1}, the average extinction coefficient of particles in the range of 0.5-2.0 μm was 0.50 km^{-1}, and the average extinction coefficient of particles > 2.0 μm was 0.16 km^{-1}.

b. Remote sensing retrieval of microphysical features of fog

There are many studies on microphysical parameters of fog inversion from satellite data. Wu et al. (2005) used MODIS data for the inversion of the total vertical water vapor content (LWP) and effective radius of fog droplets for the fogs in north of Xinjiang. The peak value of LWP was 12 g m^{-2} and varied in the range of 6-16 g m^{-2}. The effective radius of fog droplets varied widely in the range of 4-50 μm. The droplet spectrum exhibits a single peak structure with a peak value of 30 μm.

Based on the inversion of sea fog in the Yellow Sea from MODIS satellite data, Zhang et al. (2009) derived quantitative characteristic quantities, such as optical thickness, liquid water path, effective radius, top height of fog, and visibility. The optical thickness is large in the south and east of the Yellow Sea, and the optical thickness is small in the central Yellow Sea. The liquid water path in the south and east of the Yellow Sea is greater than that in the central Yellow Sea; the effective radius is large in the central region (> 9 μm), and the effective radius in the east and south is small (approximately 3 μm). The top height of the fog is essentially 100-200 m; it is relatively high in the east and south and is low in the central region. When a ship sailed in sea fog with the visibility below 200 m, the result retrieved from satellite data indicated that the visibility at the location of the ship was 100-150 m. Therefore, the inversion result and ship-measured data are roughly consistent.

Liu et al. (2010b) used the multi-spectral data of NOAA/AVHRR to retrieve three cases of cold fog, water fog and sea advection fog during 24-27 December 2006 and generated the effective radius of the fog droplets. They used the characteristic quantities of visible reflectance, temperature and the effective radius of fog droplets to quantitatively analyze microphysical characteristics of the fog top. The visible reflectance of the three types of fog was 30-60%. The visible reflectance of relatively thick fog was very high, and the effective radius of the fog was small (7-10 μm), with a relatively stable value. In comparison with stratiform clouds, the brightness temperature of the fog top was relatively high, and the fog-top brightness temperature of sea advection fog was higher than the surrounding sea surface temperature. Based on comparison with ground observations, the retrieved effective radius of the fog droplets is reasonable, which indicates that the inversion results are reliable.

c. Numerical simulations and studies of fog microphysics

(1) Model studies on the physical and chemical processes of fog

Jia and Guo (2012) used the WRF/Chem model in combination with the inventory of source emission to study the activation effect of secondary aerosols (e.g., SO_4^{-2}, NO_3^- and NH_4^+) in fog process. Many secondary aerosols are activated as condensation nuclei in clouds through NO_3^-, SO_4^{-2} and NH_4^+, and participate in the formation of fog. The average activation rates of SO_4^{-2}, NO_3^- and NH_4^+ are 34%, 31% and 30%, respectively, and the maximum activation rates are 62%, 86% and 55%, respectively. Approximately 1/3 of secondary aerosols participate in the formation of fog, and this percentage will be even higher if water vapor condition is adequate.

Based on the equilibrium equation for particle groups of discrete systems, Ding et al. (2012) adopted the multiple Monte Carlo algorithms for a numerical study of multi-effect kinetic events of aerosol particles in the fog layer during the fog-haze transformation process. They found that at the stage of fog formation, the coagulation and condensation effects of aerosols caused many small particles to transform into relatively large particles. In the fog development stage, under the combined action of multiple kinetic events (e.g., condensation, collision, deposition, and nucleation), the total number of aerosol particles and the average volume of particles changed slowly with time, and the number of particles was relatively large for aerosol particles with a volumetric size of 17.4. At the stage of fog dissipation, because crushing, evaporation and deposition effects of aerosols dominated, the volumetric size of the aerosol particles gradually declined, and the number of particles gradually increased. The number of particles with a volumetric size of 0.0156 was 8.12 times the initial value, which indicates that when fog dissipated, a large number of aerosol particles were left suspended in the atmosphere.

(2) Modeling studies of moderate- and small-scale fog

The modeling of microphysical processes of fog in China began with a one-dimensional fog model in 1992 (Peng and Li, 1992). The model included the momentum equation, heat equation, water vapor equation, and equations of droplet condensation growth and variation of number concentration, and adopted a classification technique. The model considered the impact of radiation cooling of fog droplets on condensation growth, which reduces the saturation condition for the growth of fog droplets or even allows condensation to grow in unsaturated air because the surface of fog droplets reaches saturation. In the calculation of microphysical processes, it is considered that the characteristic features of condensation growth of fog droplets is that the growth of small droplets is fast, while the growth of large droplets is slow. Therefore, the model presumes that LWC has been absorbed to become solution droplets before the condensation and growth of all CCNs (Cloud Condensation Nuclei) and transforms to fog droplets when it begins to grow. Then, gradual improvements have been made in the two-dimensional (Zhang and Li, 1993) and three-dimensional fog models (Shi al., 1997).

Li et al. (2002) introduced the microphysical features of fog into the numerical model of water-mist diffusion, and the results indicated that after introducing fog droplet spectrum into the model, the range of water-mist diffusion and the range of relative humidity change became closer to the measurements in comparison with the case without considering fog droplet spectrum. The subsequent mesoscale numerical models selected different schemes of microphysical parameterization

(Shi et al., 2005; Dong et al., 2006; He et al., 2009a, 2009b). He et al. (2009a) suggested that higher vertical resolution of the model and finer microphysical scheme of clouds can significantly improve the results of radiation fog simulation.

d. Microphysical changes in artificial fog dispersal experiments

In recent years, experiments in artificial fog dispersal have been conducted. For instance, Jin et al. (2013) used the approach of tobacco combustion to seed a hygroscopic flame agent to catalyze warm fog and used the approach of seeding liquid nitrogen to implement an anti-fogging experiment on cold fog. Analyzing fog microphysical observation data during these two anti-fogging experiments, the authors indicated that the fog responded considerably to the artificial catalysis: the concentration of fog droplets first increased and then decreased, with intense variation; the characteristic microphysical quantities, such as LWC and size of fog droplets, also exhibited significant changes. During the period of catalysis, the fog droplet spectrum exhibited broadening, and the spectral width was restored to the pre-catalytic state after the catalysis was over; the catalysis effect led to the appearance of fog at different development stages, and the fog droplet spectrum underwent a transformation between single-peak distribution and double-peak distribution: The fog droplet size distribution (DSD) was unimodal before seeding and bimodal during seeding. The bimodal DSD appeared again and again for several times and they all kept for little time. The fog DSD changed gradually from continuous simple decrease DSD to unimodal DSD and bimodal DSD after the first bimodal DSD appeared. DSD changed back to be unimodal from bimodal after the seeding was over. The analysis indicated that the ripening process occurred in the warm fog after catalysis, whereas the cold-fog catalysis initiated the Bergeron process (Jin et al., 2013).

8. Prospects and conclusions

This review demonstrated that, in the past 50 years, fog microphysics studies related to various aspects were carried out in China, and great achievements were made, however, the research about the fog microphysics still lags behind that of Europe, the United States and other advanced economies.

We believe in the near future, the following several aspects need to strengthen: (1) The measurements of fog microstructure characteristics: extensive fog microphysics measurements are needed, although there are many efforts focusing on fog microphysics, their physical understanding is still in question in different cases and different environments. (2) The fog-haze transformation microphysical processes and mechanisms need be revealed. Most of the past researches divided the fog and the haze, however the haze transformed to fog need further observation and analysis. (3)The fog spectral widening is another question need to be revealed. Since the explosive features would appear in larger areas, the synchronous observations in larger ranges would be carried out in the future. (4) The relationship between fog microphysics, radiation, nocturnal boundary layer, turbulence, and pollutions need to be further uncovered. (5) Artificial influence fog microstructure could achieve the goal of weakening or even dispersing fog and haze. (6) Further studies could use the acquired microphysical parameters to improve the numerical models which could further improve the fog forecast.

Future efforts related to the issues summarized above would be extremely helpful to our better understanding of fog microphysical and related processes and fog forecasting issues.

Acknowledgements. Funding for this work was jointly provided by the National Key Project of MOST (JFYS2016ZY01-002213-03), the Natural Science Foundation of Jiangsu Province (Grant No. BK20130111), the National Natural Science Foundation of China (41575135, 91544229 and 91544231) and the Key Projects of Jiangsu Meteorological Bureau (Grant No. KZ201405). China Scholarship Council Program, and the Youth Talent Plan of the China Meteorological Administration.

Edited by: Chun-Chieh Wu

References

Bao, B. T., J. X. Shu, and B. Q. Zhu, 1995: Study on physicochemical properties of urban fog in Shanghai. *J. Nanjing Inst. Meteor.*, **18**, 114-118 (in Chinese with English abstract).

Deng, X. J., D. Wu, and Y. X. Ye, 2002: Physical characteristics of dense fog at Nanling Mountain region. *J. Trop. Meteorol.*, **18**, 227-236 (in Chinese with English abstract).

______, ______, H. H. Tang, S. J. Fan, H. H. Huang, W. K. Mao, and Y. X. Ye, 2007a: Analyses on boundary layer structure of a frontal heavy fog process in Nanling Mountain area. *Plateau Meteorol.*, **26**, 881-889 (in Chinese with English abstract).

______, ______, Y. Q. Shi, H. H. Tang, S. J. Fan, H. H. Huang, W. K. Mao, and Y. X. Ye, 2007b: Comprehensive analysis of the macro-and micro-physical characteristics of dense fog in the area south of the Nanling Mountains. *J. Trop. Meteorol.*, **23**, 424-434 (in Chinese with English abstract).

Dilnur, T., A. Ablikim, and Z. C. Pu, 2008: The chemical character of fog water at Nanshan in Urumqi. *J. Xinjiang Univ.*, **25**, 330-333 (in Chinese with English abstract).

Ding, J., Y. Liu, J. H. Li, B. L. Zhang, and Q. T. Wang, 2012: Dynamical characteristics of aerosol particles from fog to haze weather. *J. Meteorol. Environ.*, **28**, 91-96 (in Chinese with English abstract).

Ding, Y. H., and Y. J. Liu, 2014: Analysis of long-term variations of fog and haze in China in recent 50 years and their relations with atmospheric humidity. *Sci. China Earth Sci.,* **57**, 36-46, doi:10.1007/s11430-013-4792-1.

Dong, J. X., H. C. Lei, Z. X. Hu, W. A. Xiao, and X. Q. Zhang, 2006: Numerical simulation and diagnosis of a dense fog in Beijing and its penumbra. *Climatic Environ. Res.*, **11**, 175-184 (in Chinese with English abstract).

Fan, Q., A. Y. Wang, S. J. Fan, D. Wu, and J. J. Liang, 2004: Numerical simulation study of a radiation fog in Pearl River Delta regions. *Sci. Meteorol. Sin.*, **24**, 1-8 (in Chinese with English abstract).

Fu, G., T. Zhang, and F. Zhou, 2002: Three-dimesional numerical simulation of real sea fog event over the Yellow Sea. *J. Ocean Univ. Qingdao*, **32**, 859-867 (in Chinese with English abstract).

______, J. Q. Wang, M. G. Zhang, J. T. Guo, M. K. Guo, and K. C. Guo, 2004: An observational and numerical study of a sea fog event over the Yellow Sea on 11 April, 2004. *J. Ocean Univ. Qingdao,* **34**, 720-726 (in Chinese with English abstract).

Fu, G. Q., W. Y. Xu, R. F. Yang, J. B. Li, and C. S. Zhao, 2014: The distribution and trends of fog and haze in the North China Plain over the past 30 years. *Atmos. Chem. Phys.,* **14**, 11949-11958, doi:10.5194/acp-14-11949-2014.

Gong, S. X., and S. H. Ling, 1996: Fog decreasing in Xishuangbanna region, China. *Meteorol. Mon.,* **22**, 10-14 (in Chinese with English abstract).

Gu, Z. C., 1962: Recent investigations in the theory of the formation of the cloud-drop spectra. *Acta Meteorol. Sin.,* **32**, 267-284 (in Chinese with English abstract).

______, 1980: *Cloud Precipitation Physical Basis*. science press, 219 pp (in Chinese).

______, and G. X. Hu, 1962: A linear theory of the influence of condensation feedback on the development of the cloud. *Acta Meteorol. Sin.,* **32**, 64-70 (in Chinese).

______, and L. S. Zhan, 1962: On the growth of the droplets under gravitational coalescence in a fluctuating environment. *Acta Meteorol. Sin.,* **32**, 301-307 (in Chinese).

______, and ______, 1964: On the gravitational coalescence growth of the cloud droplets in a cloud with fluctuating water content. *Sci. China Ser. A*, **4**, 129-135 (in Chinese with English abstract).

Gultepe, I., and Coauthors, 2007: Fog research: A review of past achievements and future perspectives. *Pure Appl. Geophys.*, **164**, 1121-1159, doi:10.1007/s00024-007-0211-x.

Guo, E. M., X. R. Yu, and Y. H. Li, 1989: A study on macro-and micro-structures of fog in Shuangliu airport. *Proc. National Cloud Physics and Weather Modication Conf.,* Huhhot, Mongolia, Committee of Atmos. Phys. Chinese Meteor. Soc., 35-35 (in Chinese with English abstract).

______, Y. G. Liu, and J. Shu, 1990: A study on macro-and micro-structures of fog in Huangpu River. *J. Beijing Inst. Meteor.*, **1**, 46-49 (in Chinese with English abstract).

He, H., H. Jin, J. Z. Liu, T. M. Zhang, and Y. H. Gao, 2009a: Simulation and analysis of a radiation fog event in Beijing area. *Climatic Environ. Res.*, **14**, 390-398 (in Chinese with English abstract).

______, X. L. Guo, J. Z. Liu, H. Jin, and S. J. Lou, 2009b: Observation and simulation study of the boundary layer structure and the formation, dispersal mechanism of a heavy fog event in Beijing area. *Chinese J. Atmos. Sci.*, **33**, 1174-1186 (in Chinese with English abstract).

Huang, H. J., J. Huang, W. K. Mao, F. Liao, X. N. Li, W. H. Lu, and Y. Q. Yang, 2009: Characteristics of liquid water content of sea fog in Maoming area and its relationship with atmospheric horizontal visibility. *Acta Oceanol. Sin.*, **32**, 40-53 (in Chinese with English abstract).

Huang, J. P., Q. Y. Mei, Y. C. Jin, and Z. H. Li, 1998: Micirophysical structure features and evolution processes of radiation fog in Huning region. *Meteorol. Mon.,* **24**, 3-8 (in Chinese with English abstract).

______, Z. H. Li, Y. R. Huang, and Y. S. Huang, 2000: A three-dimensional model study of complex terrain fog. *Chinese J. Atmos. Sci.*, **24**, 821-834 (in Chinese with English abstract).

Huang, P. Q., and L. Guo, 1986: Numerical simulation of radiation fog formation. *Sci. Meteorol. Sin.*, **4**, 68-74 (in Chinese with English abstract).

Huang, Y. R., Y. Shen, Y. S. Huang, and Y. Z. Tan, 2001: Effects of urbanization on radiation fog in Xishuangbanna area. *Plateau Meteorol.*, **20**, 186-190 (in Chinese with English abstract).

Huang, Y. S., W. R. Xu, Z. H. Li, L. Fan, and W. J. Huang, 1992: An observation and analysis on the radiation fog in Xishuangbanna. *Acta Meteorol. Sin.,* **50**, 112-117 (in Chinese with English abstract).

______, Y. R. Huang, Z. H. Li, B. J. Chen, J. P. Huang, and J. X. Gu, 2000: The microphysical structure and evolution of winter fog in Xishuangbanna. *Acta Meteorol. Sin.,* **58**, 715-725 (in Chinese with English abstract).

Jia, X. C., and X. L. Guo, 2012: Impacts of secondary aerosols on a persistent fog event in Northern China. *Atmos. Ocean. Sci. Lett.*, **5**, 401-407, doi10.1080/16742834.2012.11447022.

Jiang, Y. H., Q. Wang, Z. H. Li, and L. Ma, 1994: Characteristics of fog in Chongqing urban area. *Meteorol. Sci. Technol*., **32**, 450-455 (in Chinese with English abstract).

Jin, H., H. He, Q. Zhang, M. Y. Huang, X. C. Ma, L. Zhang, and L. Ji, 2013: Analyses of a microphysical response to the seeding in two artificial fog dissipation. *J. Trop. Meteorol*., **19**, 357-366, doi:1006-8775(2013) 04-0357-10.

Koračin, D., C. E. Dorman, J. M. Lewis, J. G. Hudson, E. M. Wilcox, and A. Torregrosa, 2014: Marine fog: A review. *Atmos. Res.*, **143**, 142-175, doi:10.1016/j.atmosres.2013.12.012.

Li, M., W. M. Jiang, and H. N. Liu, 2002: A numerical simulation study of atmospheric transport and dispersion of the spray with considering the microphysics characteristic. *Acta Scientiae Circumstantiae*, **22**, 140-144 (in Chinese with English abstract).

Li, X. B., C. W. Gong, C. Li, C. D. Xu, X. H. Chen, Q. S. Xu, and H. L. Wei, 2009: Size distribution and attention for infrared radiation of fog particles. *Laser. Infrared*, **39**, 742-745 (in Chinese with English abstract).

Li, Z. H., 2001: Studies of fog in China over the past 40 years. *Acta Meteorol. Sin.,* **59**, 616-624 (in Chinese with English abstract).

______, and Z. G. Peng, 1994: Physical and chemical characteristics of the Chongqing winter fog. *Acta Meteorol. Sin.,* **52**, 477-483 (in Chinese with English abstract).

______, and J. Wu, 1995: Winter fog droplet spectrum features in urban area of Chongqing. *J. Nanjing Inst. Meteor.*, **18**, 46-51 (in Chinese with English abstract).

______, L. X. Zhong, and X. R. Yu, 1992: The temporal-spatial distribution and physical structure of land fog in southwest China and the Changjiang River Basin. *Acta Geogr. Sin.*, **47**, 245-251 (in Chinese with English abstract).

______, J. P. Huang, and Y. Q. Zhou, 1999: Physical structures of the five-day sustained fog around Nanjing in 1996. *Acta Meteorol. Sin.,* **57**, 622-631 (in Chinese with English abstract).

______, D. Y. Liu, and J. Yang, 2011a: The microphysical processes and macroscopic conditions of the radiation fog droplet spectrum broadening. *Chinese J. Atmos. Sci.*, **35**, 41-54 (in Chinese with English abstract).

______, D. Y. Liu, J. Yang, and M. J. Pu, 2011b: Physical and chemical characteristics of winter fogs in Nanjing. *Acta Meteorol. Sin.,* **69**, 706-718 (in Chinese with English abstract).

______, J. Yang, C. E. Shi, and M. J. Pu, 2012: Urbanization effects on fog in china: Field research and modeling. *Pure Appl. Geophys.*, **169**, 927-939, doi:10.1007/s00024-011-0356-5.

Liu, C. S., and W. B. Liu, 1979: The measurements of size distribution of fog droplets by laser holography. *J. Nanjing Univ.*, **15**, 77-83 (in Chinese with English abstract).

Liu, D. Y., 2011: Observational Study on the Winter Fog Macro- Micro-Physical Structures in Nanjing. Ph.D. Thesis, Nan Jing University of Information Science & Technology, 115 pp (in Chinese with English abstract).

______, J. Yang, S. J. Niu, and Z. H. Li, 2011: On the evolution and structure of a radiation fog event in Nanjing. *Adv. Atmos. Sci.*, **28**, 223-237, doi:10.1007/s00376-010-0017-0.

______, S. J. Niu, J. Yang, L. J. Zhao, J. J. Lu, and C. C. Lu, 2012a: Summary of a 4-year fog field study in northern Nanjing, part 1: Fog boundary layer. *Pure Appl. Geophys.*, **169**, 809-819, doi:10.1007/

s00024-011-0343-x.
______, M. J. Pu, J. Yang, G. Z. Zhang, W. L. Yan, and Z. H. Li, 2010a: Microphysical structure and evolution of a four-day persistent fog event in Nanjing in December 2006. *Acta Meteorol. Sin.,* **24**, 104-115.
______, W. L. Yan, J. Yang, M. J. Pu, S. J. Niu, and Z. H. Li, 2016: A study of the physical processes of an advection fog boundary layer. *Bound.-Layer Meteor.*, **158**, 125-138, doi:10.1007/s10546-015-0076-y.
Liu, G. H., X. Yu, and Z. G. Yue, 2010b: Analysis of fog microphysical parameters from NOAA/AVHRR images. *Sci. Meteorol. Sin.*, **30**, 846-850 (in Chinese with English abstract).
Liu, L. W., S. J. Niu, D. Y. Liu, and C. S. Lu, 2012b: Evolution characteristics and burst reinforcement of winter dense fog in Nanjing. *Trans. Atmos. Sci.*, **35**, 103-112 (in Chinese with English abstract).
Lu, C. S., S. J. Niu, J. Yang, and W. W. Wang, 2008: An observational study on physical mechanism and boundary layer structure of winter advection fog in Nanjing. *J. Nanjing Inst. Meteor.*, **31**, 520-529 (in Chinese with English abstract).
______, ______, ______, X. Liu, and L. J. Zhao, 2010a: Jump features and causes of macro and microphysical structures of a winter fog in Nanjing. *Chinese J. Atmos. Sci.*, **34**, 681-690 (in Chinese with English abstract).
______, ______, L. L. Tang, J. J. Lu, L. J. Zhao, and B. Zhu, 2010b: Chemical composition of fog water in Nanjing area of China and its related fog microphysics. *Atmos. Res.,* **97**, 47-69, doi:10.1016/j.atmosres.2010.03.007.
______, ______, P. Yue, Z. G. Yue, and L. Xiang, 2011: Observational research on boundary layer structure during high incidence period of winter fog in Nanjing. *Trans. Atmos. Sci.*, **34**, 58-65 (in Chinese with English abstract).
Lu, J. J., S. J. Niu, L. J. Zhao, Y. Zhang, and F. Xu, 2014a: Microphysical characteristics of a sea fog influenced by a cold front in Zhanjiang. *Trans. Atmos. Sci.*, **37**, 208-215 (in Chinese with English abstract).
______, ______, Y. Zhang, and F. Xu, 2014b: Evolution characteristics of the macro-/micro- structure and the boundary layer during a spring heavy sea fog episode in Donghai Island in Zhanjiang. *Acta Meteorol. Sin.,* **72**, 350-365 (in Chinese with English abstract).
Ma, Z. Q., X. J. Zhao, W. Meng, Y. J. Meng, D. He, and H. Y. Liu, 2012: Comparison of influence of fog and haze on visibility in Beijing. *Res. Environ. Sci.*, **25**, 1208-1214 (in Chinese with English abstract).
Niu, S. J., C. S. Lu, Y. G. Liu, L. J. Zhao, J. J. Lu, and J. Yang, 2010a: Analysis of the microphysical structure of heavy fog using a droplet spectrometer: A case study. *Adv. Atmos. Sci.*, **27**, 1259-1275, doi: 10.1007/s00376-010-8192-6.
______, ______, H. Y. Yu, L. J. Zhao, and J. J. Lu, 2010b: Fog research in China: An overview. *Adv. Atmos. Sci.*, **27**, 639-662, doi:10.1007/s00376-009-8174-8.
______, D. Y. Liu, L. J. Zhao, C. S. Lu, J. J. Lu, and J. Yang, 2012: Summary of a 4-year fog field study in northern Nanjing, part 2: Fog microphysics. *Pure Appl. Geophys.*, **169**, 1137-1155, doi:10.1007/s00024-011-0344-9.
Pandis, S. N., J. H. Seinfeld, and C. Pilinis, 1992: Heterogeneous sulfate production in an urban fog. *Atmos. Environ. A-Gen.*, **26**, 2509-2522, doi:10.1016/0960-1686(92)90103-R.
Peng, H., and Z. H. Li, 1992: One-dimension numerical model of radiation fog with detailed microphysics. *Chongqing Environ. Sci.*, **14**, 49-54 (in Chinese with English abstract).
Pu, M. J., G. Z. Zhang, W. L. Yan, and Z. H. Li, 2008: Features of a rare advection-radiation fog event. *Sci. China Ser. D.,* **51**, 1044-1052, doi: 10.1007/s11430-008-0071-y.
Sheng, L. F., W. F. Liang, W. J. Qu, and K. Luo, 2011: Relationship of aerosol size distribution and visibility in a sea fog. *J. Ocean Univ. Qingdao*, **41**, 1-8 (in Chinese with English abstract).
Sheng, P. X., J. T. Mao, J. G. Li, A. C. Zhang, J. G. Sang, and N. X. Pan, 2003: *Atmospheric Physics*. Beijing University Press, 522 pp (in Chinese).
Shi, C. E., J. Yang, X. J. Sun, Z. Y. Liang, and Z. H. Li, 1997: 3D model study on fog for complicated terrain. *J. Nanjing Inst. Meteor.*, **20**, 308-317 (in Chinese with English abstract).
_____, K. Y. Yao, and L. Ma, 2001: Numerical studies of effects of aerosols on urban fog. *Clim. Environ. Res.*, **6**, 485-492 (in Chinese with English abstract).
Shi, H. Y., H. F. Wang, L. L. Qi, and J. Bai, 2005: Numerical simulation of radiation fog event in Yangtze River. *J. PLA Univ. Sci. Technol.*, **6**, 404-408 (in Chinese with English abstract).
Sun, X. D., H. Y. Xu, G. C. Li, and M. Y. Huang, 1991: Two-dimension numerical model of advection-radiation fogs. *Chinese J. Atmos. Sci.*, **15**, 99-109 (in Chinese with English abstract).
Tang, H. H., S. J. Fan, D. Wu, and X. J. Deng, 2002: Research of the microphysical structure and evolution of dense fog over Nanling Mountain Area. *ACTA Sci. Nat. Univ. Sunyat.*, **41**, 92-96 (in Chinese with English abstract).
Teng, H. C., J. Yang, D. Y. Liu, and W. Zheng, 2014: Ensemble forecast of visibility based on WRF and one-dimensional fog model: A case study. *Trans. Atmos. Sci.,* **37**, 99-107 (in Chinese with English abstract).
Wang, G. C., 1981: An analysis of the microphysical structure of fog. *Acta Meteorol. Sin.,* **39**, 452-459 (in Chinese with English abstract).
Wu, B. G., H. S. Zhang, C. C. Zhang, Z. Y. Wang, L. L. Yu, B. X. Liu, and Y. Y. Xie, 2008: Analysis of the micro-meteorologic element during the advection fog period in the South of Tianjin City. *Acta Sci. Nat. Univ. Pekinensi*, **44**, 744-750 (in Chinese with English abstract).
______, ______, ______, H. Zhu, and Z. Y. Wang, 2010: Meteorological characteristics of surface layer during fog events in the urban area of Tianjin. *Clim. Environ. Res.*, **15**, 179-190 (in Chinese with English abstract).
Wu, D., X. J. Deng, S. J. Fan, Y. X. Ye, W. K. Mao, H. H. Huang, and H. H. Tang, 2005: Rain-water chemical composition of frontal rainfall in fog-sector at Dayaoshan of the Nanling Mountains. *Acta Sci. Nat. Univ. Sunyat.*, **44**, 105-109 (in Chinese with English abstract).
______, and Coauthors, 2006: Forecast system of visibility at speedway foggy area at Nanling Mountains. *J. Trop. Meteorol.*, **22**, 417-422 (in Chinese with English abstract).
______, B. Zhao, X. J. Deng, X. Y. Bi, and S. J. Fan, 2007a: A study on bad visibility over foggy section of freeway in Nanling Mountainous Region. *Plateau Meteorol.*, **26**, 649-654 (in Chinese with English abstract).
______, X. J. Deng, J. T. Mao, W. K. Mao, Y. X. Ye, X. Y. Bi, H. H. Tang, and Q. L. Wan, 2007b: A study on macro-and micro-structures of heavy fog and visibility at freeway in the Nanlingdayaoshan Mountain. *Acta Meteorol. Sin.,* **65**, 406-415 (in Chinese with English abstract).
Wu, X. J., Y. H. Chen, and S. M. Li, 2005: Utilizing MODIS data to retrieve the visibility and microphysical properties of fog happens in the northwest China. *J. Remote Sens.*, **9**, 688-696 (in Chinese with English abstract).
Xu, H. Y., and Z. C. Gu, 1963: On the formation of the precipitation element in a shallow warm-cloud. *Acta Meteorol. Sin.,* **33**, 108-114 (in Chinese with English abstract).
Xu, J. Q., Z. Zhang, and H. Wei, 1994: Measurement and analysis of droplet spectrum and liquid water content of sea fog. *Trans. Oceanol. Limnol.*, **2**, 174-178 (in Chinese with English abstract).
Yang, J., Y. J. Xie, C. E. Shi, D. Y. Liu, S. J. Niu, and Z. H. Li, 2009: Differences in ion compositions of winter fog-water between radiation and advection-radiation fog episodes in Nanjing. *Trans. Atmos. Sci.*, **32**, 776-782 (in Chinese with English abstract).
______, L. Wang, D. Y. Liu, and Z. H. Li, 2010a: The boundary layer structure and the evolution mechanisms of a deep dense fog event. *Acta Meteorol. Sin.,* **68**, 998-1006 (in Chinese with English abstract).

______, Z. Q. Niu, C. E. Shi, D. Y. Liu, and Z. H. Li, 2010b: Microphysics of atmospheric aerosols during winter haze/fog events in Nanjing. *Environ. Sci.*, **31**, 1425-1431 (in Chinese with English abstract).

______, Y. J. Xie, C. E. Shi, D. Y. Liu, S. J. Niu, and Z. H. Li, 2012: Ion composition of fog water and its relation to air pollutants during winter fog events in Nanjing, China. *Pure Appl. Geophys.*, **169**, 1037-1052, doi:10.1007/s00024-011-0342-y.

Yang, L. S., 1985: A preliminary observations of the microphysical structure of fog in Qingdao area. *Marine Sci.*, **9**, 49-50 (in Chinese with English abstract).

Yang, Z. Q., S. Z. Xu, and B. Geng, 1989: Formation and microphysical structures of spring sea fog in Zhoushan area. *Acta Oceanol. Sin.*, **11**, 431-438 (in Chinese with English abstract).

You, H., M. Yang, R. F. Guo, and X. W. Bai, 2008: Diagnostic analysis of typical mountainous fog process in Eshan along Kunming-Daluo High way in Yunnan. *Meteorol. Mon.*, **34**, 87-94 (in Chinese with English abstract).

Yu, X. R., and M. Su, 1990: Research and analysis of Yangtze River Basin fog. *Meteorol. Mon.,* **33**, 119-123 (in Chinese with English abstract).

Yue, Y. Y., S. J. Niu, L. J. Zhao, Y. Zhang, and F. Xu, 2012: Chemical composition of sea fog water along the South China Sea. *Pure Appl. Geophys.*, **169**, 2231-2249, doi:10.1007/s00024-012-0486-4.

______, ______, ______, ______, and ______, 2013: Study on the synoptic system and macro-micro characteristics of sea fog along the Zhanjiang coastal area. *Chinese J. Atmos. Sci.*, **37**, 609-622 (in Chinese with English abstract).

______, ______, ______, ______, and ______, 2014: The influences of macro- and microphysical characteristics of sea-fog on fog-water chemical composition. *Adv. Atmos. Sci.*, **31**, 624-636, doi:10.1007/s00376-013-3059-2.

Zhang, G. Z., L. G. Bian, J. Z. Wang, Y. Q. Yang, W. Q. Yao, and X. D. Xu, 2005: The boundary layer characteristics in the heavy fog formation process over Beijing and its adjacent areas. *Sci. China Ser. D.,* **48**, 88-101, doi:10. 1360/05yd0029.

Zhang, J. W., S. P. Zhang, X. J. Wu, Y. C. Liu, and J. W. Liu, 2009: The research on Yellow sea fog based on MODIS data: sea fog properties retrieval and spatial-temporal distribution. *J. Ocean Univ. Qingdao*, **39**, 311-318 (in Chinese with English abstract).

Zhang, L. M., and Z. H. Li, 1993: A two-dimensional time-integral numerical model of Chongqing fog. *Chinese J. Atmos. Sci.*, **17**, 750-755 (in Chinese with English abstract).

Zhang, S. P., and X. W. Bao, 2008: The main advances in sea fog research in China. *J. Ocean Univ. Qingdao,* **38**, 359-366.

Zhang, S. T., S. J. Niu, and L. J. Zhao, 2013: The microphysical structure of fog droplets in a sea fog event in the South China Sea. *Chinese J. Atmos. Sci.,* **37**, 552-562 (in Chinese with English abstract).

Zhao, L. J., S. J. Niu, Y. Zhang, and F. Xu, 2013: Microphysical characteristics of sea fog over the east coast of Leizhou Peninsula, China. *Adv. Atmos. Sci.*, **30**, 1154-1172, doi:10.1007/s00376-012-1266-x.

Zhou, B. B., 1987: The numerical modeling of radiation fog. *Acta Meteorol. Sin.,* **45**, 21-29 (in Chinese with English abstract).

______, ______, B. S. Deng, and H. G. Xu, 2004: Numerical simulation on the boundary layer structure during a heavy fog process over Beijing metropolitan area. *Acta Meteorol. Sin.,* **62**, 468-475 (in Chinese with English abstract).

Zhou, X. J., 1963: Statistical theory on the mechanism of microscopic physical warm cloud precipitation. *Acta Meteorol. Sin.,* **33**, 97-107 (in Chinese).

______, and Z. C. Gu, 1963: Theories of fog-cloud microstructure and precipitation process. *Chinese Sci. Bull.*, **8**, 1-7 (in Chinese).